Experimental Neurology 278 (2016) 42–53

Contents lists available at ScienceDirect

Experimental Neurology

journal homepage: www.elsevier.com/locate/yexnr

# Anti-glycan antibodies halt axon regeneration in a model of Guillain Barrè Syndrome axonal neuropathy by inducing microtubule disorganization via RhoA–ROCK-dependent inactivation of CRMP-2

Victoria Rozés Salvador [a], Florencia Heredia [a], Andrés Berardo [a], Anabela Palandri [a], Jose Wojnacki [a], Ana L. Vivinetto [a], Kazim A. Sheikh [c], Alfredo Caceres [a], Pablo H.H. Lopez [a,b,*]

[a] Laboratory of Neurobiology, Instituto de Investigación Médica Mercedes y Martin Ferreyra, INIMEC-CONICET-Universidad Nacional de Córdoba, Argentina
[b] Facultad de Psicología, Universidad Nacional de Córdoba, Argentina
[c] Department of Neurology, University of Texas Medical School at Houston, Houston, USA

ARTICLE INFO

*Article history:*
Received 14 January 2016
Accepted 19 January 2016
Available online 22 January 2016

*Keywords:*
Ganglioside
Nerve repair
Axon regeneration
Guillain Barrè Syndrome
Anti-glycan antibodies
RhoA GTPase
Peripheral nerve

ABSTRACT

Several reports have linked the presence of high titers of anti-Gg Abs with delayed recovery/poor prognosis in GBS. In most cases, failure to recover is associated with halted/deficient axon regeneration. Previous work identified that monoclonal and patient-derived anti-Gg Abs can act as inhibitory factors in an animal model of axon regeneration. Further studies using primary dorsal root ganglion neuron (DRGn) cultures demonstrated that anti-Gg Abs can inhibit neurite outgrowth by targeting gangliosides via activation of the small GTPase RhoA and its associated kinase (ROCK), a signaling pathway common to other established inhibitors of axon regeneration. We aimed to study the molecular basis of the inhibitory effect of anti-Gg abs on neurite outgrowth by dissecting the molecular dynamics of growth cones (GC) cytoskeleton in relation to the spatial–temporal analysis of RhoA activity. We now report that axon growth inhibition in DRGn induced by a well characterized mAb targeting gangliosides GD1a/GT1b involves: i) an early RhoA/ROCK-independent collapse of lamellipodia; ii) a RhoA/ROCK-dependent shrinking of filopodia; and iii) alteration of GC microtubule organization/and presumably dynamics via RhoA/ROCK-dependent phosphorylation of CRMP-2 at threonine 555. Our results also show that mAb 1B7 inhibits peripheral axon regeneration in an animal model via phosphorylation/inactivation of CRMP-2 at threonine 555. Overall, our data may help to explain the molecular mechanisms underlying impaired nerve repair in GBS. Future work should define RhoA-independent pathway/s and effectors regulating actin cytoskeleton, thus providing an opportunity for the design of a successful therapy to guarantee an efficient target reinnervation.



## 1. Introduction

Axon regeneration is the first critical step for the restoration of structure and function following nerve lesions in the peripheral nervous system. Successful reconnection with end-target organs requires appropriate axon growth and pathfinding to guarantee efficient and proper reinnervation. Axon regeneration and target reinnervation are commanded by growth cones (GCs), specialized structures located at neuritic tips that provide actin-guided extension of microtubules (MTs) required for axon extension (Gordon-Weeks, 1987; Bradke et al., 2012). GCs are the target of molecules that halt axon regeneration, including anti-ganglioside antibodies (anti-Gg Abs) associated with human acute immune neuropathies, such as Guillain Barrè Syndrome (GBS) (Yuki and Hartung, 2012). Several clinical studies have associated the presence of anti-Gg Abs with poor/delayed clinical recovery in GBS (Carpo et al., 1999; Press et al., 2001; Ilyas et al., 1992; Gregson et al., 1993; Simone et al., 1993; Jacobs et al., 1996; Bech et al., 1997; Kuwabara et al., 1998; Annunziata et al., 2003; Koga et al., 2003). In most cases, incomplete clinical recovery involves failure of nerve regeneration and target denervation (Brown and Feasby, 1984). A direct inhibitory role of anti-Gg Abs on axon regeneration has been demonstrated in cultured neurons and in an animal model of peripheral nerve regeneration using either monoclonal antibodies (mAbs) or

*Abbreviations:* GBS, Guillain Barrè Syndrome; DRGn, dorsal root ganglion neurons; MTs, microtubules; DRG, dorsal root ganglion; GC, growth cone; CRMP-2, collapsing response mediator protein 2; intraperitoneally, IP; IgG, immunoglobulin G; tubulin GFP, green fluorescent protein (GFP)-tagged α-tubulin; CRMP-2 T555A, mutant form of CRMP-2 at residue 555 (threonine → alanine); $p75^{NTR}$, low affinity receptor for neurothrophins p75; Rho-GDIα, Rho-GDP dissociation inhibitor α; ROCK, Rho-associated kinase; FRET, Förster resonance energy transfer; mAbs, monoclonal antibodies; 1B7, anti-GD1a/GT1b IgG2b mAb; Gg, ganglioside; TUJ-1, mAb against class III β-tubulin; TAT-C3, cell permeable exoenzyme C3 transferase; Y-27632, specific Rho-associated kinase inhibitor; LIMK1, LIM Domain Kinase-1; MIA, myelin-derived inhibitors of axon regeneration; MAG, myelin-associated glycoprotein.

* Corresponding author at: Laboratory of Neurobiology, Instituto de Investigación Médica Mercedes y Martin Ferreyra, INIMEC-CONICET-Universidad Nacional de Córdoba, Friuli 2434, Barrio Colinas de Vélez Sarsfield, Córdoba 5016, Provincia de Córdoba, Argentina.
*E-mail address:* phhlopez@immf.uncor.edu (P.H.H. Lopez).

http://dx.doi.org/10.1016/j.expneurol.2016.01.016
0014-4886/

patient-derived anti-Gg Abs (Lehmann et al., 2007; Lopez et al., 2010). In this model, inhibition of axon regeneration by anti-Gg Abs has been linked to the presence of end-bulb like structures characteristic of dystrophic growth cones at the lesion site (Lehmann et al., 2007). In cultured dorsal root ganglion neurons (DRGn), anti-Gg Abs inhibit neurite outgrowth by a mechanism involving cross-linking of cell surface gangliosides and subsequent activation of the small GTPase RhoA and its associated kinase (ROCK) (Zhang et al., 2011). RhoA plays a key role in the negative regulation of axon growth due to its ability to control cytoskeletal reorganization and dynamics and is identified as a major target of many inhibitors of axon regeneration (McKerracher et al., 2012; Fujita and Yamashita, 2014). ROCK has several targets including CRMP-2, a member of the dihydropyrimidinase-like or Collapsin Response Mediator Protein (CRMP) family with important roles in axon growth and microtubule assembly (Wang and Strittmatter, 1996; Khazaei et al., 2014; Tan et al., 2015). CRMP-2 binds to the α/β tubulin heterodimer promoting MT assembly while ROCK-dependent phosphorylation/inactivation of CRMP-2 at Thr-555 mediates GC collapse in DRGn (Arimura et al., 2000; Arimura et al., 2005).

Defining the molecules and signaling pathways that prevent regeneration of injured axons can provide key insights that may allow development of therapeutic approaches to enhance axon growth in neurological disease. The present study is aimed to gain novel insights into the mechanisms of anti-Gg Abs-induced inhibition of axon regeneration. We now report that axon growth inhibition induced by a well characterized mAb targeting gangliosides GD1a/GT1b (clone 1B7) involves negative modulation of the: a) Actin cytoskeleton by RhoA/ROCK-dependent (filopodia) and independent (lamellipodia) mechanisms; and b) MT cytoskeleton by a RhoA/ROCK-dependent pathway via phosphorylation/inactivation of CRMP-2 at threonine 555. These events are temporally dissociated with actin modifications, including lamellipodia retraction, preceding alterations in GC MT organization and dynamics. Overall, our data provide data that may help explain the molecular mechanisms underlying impaired nerve repair in GBS.

## 2. Materials and methods

### 2.1. DRG cultures and in vitro electroporation

Postnatal 5–7 day-old Wistar rat pups were decapitated and dorsal root ganglions (DRGs) removed. DRGs were further dissociated by treatment with 0.2% collagenase followed by 0.1% trypsin in DMEM medium and then triturated with pipette tips of decreasing diameters. The suspension was centrifuged at 100 × *g* for 1 min. Cells were resuspended in DMEM medium and plated on a 35-mm plastic petri dish for 1 h to separate the glial cells. The non-adherent cells were later plated onto coated slides (10 μg/ml poly-L-lysine and 1 μg/ml mouse laminin) in DMEM supplemented with 10% FBS, 1% penicillin–streptomycin, and glutaMAX 100× for 1 h. Then, the medium was removed and cells were maintained in Neurobasal medium supplemented with B27, glutaMAX and 50 ng/ml of nerve growth factor. Dissociated neurons were transfected with plasmid constructs with the AMAXA® Nucleofector using the Basic Neuron SCN Nucleofector® kit (Lonza) with 0.5–2 μg of DNA depending of each construct following the manufacturer's instructions.

### 2.2. Anti-ganglioside monoclonal antibody

The generation, specificity and purification of the anti-GD1a/GT1b IgG2b mAb (clone 1B7) were reported in previous studies (Lunn et al., 2000; Gong et al., 2002; Chen et al., 2014; Zhang et al., 2004), including its capacity to severely inhibit axon regeneration in an animal model (Lehmann et al., 2007). An irrelevant mouse IgG was used as a negative control Ab.

### 2.3. Treatments

Dissociated DRGn were treated 5 h post-plating with anti-GD1a/GT1b mAb or IgG control (50 μg/ml) and analyzed at different times thereafter. In experiments using Rho Inhibitor I (ADP ribosylation of Rho Asn-41, Cytoskeleton), cells were treated at 1 μg/ml for 1 h before the addition of anti-GD1a/GT1b mAb or IgG control to the cultures. For experiments with Y-27632, a Rho-associated protein kinase inhibitor (Calbiochem), cultures were treated at 2 or 10 μM concentration. DRGn cultures were pretreated 30 min with Y-27632 before the addition of anti-GD1a/GT1b mAb or IgG control. In another set of experiments DRGn were pretreated for 1 h with 10 mU/ml *Vibrio cholerae* sialidase, an enzyme that hydrolyzes sialic acids and eliminates Ab-ganglioside binding (Mehta et al., 2007).

### 2.4. DNA constructs

The cDNA sequence for human α-tubulin fused to the green fluorescent protein (tubulin-GFP) expressed from a pcDNA3 vector backbone (Invitrogen) and the F-actin biosensor LifeAct-mCherry (Ibidi®) were used for video time-lapse experiments. Constructs pXJ40FLAG carrying rat Wt CRMP-2 and its mutant form at residue 555 (CRMP-2 T555A) were kindly provided by Dr. Christine Hall (University College London, London, UK) and their use previously reported (Brown et al., 2004; Hall et al., 2001). These constructs were used for in vitro and in vivo DRGn electroporation.

### 2.5. Single-cell microinjection

DRGn were nucleofected using borosilicate glass capillaries and a buffer containing HEPES (10 mM) and KCl (140 mM) pH: 7.4. as described (Zhang and Yu, 2008).

### 2.6. Time-lapse video microscopy

Dissociated DRGn were co-nucleofected with 0.2 μg/μl tubulin-GFP and LifeAct-mCherry plasmids each. After 5 h post-nucleofection, cells were treated with anti-GD1a/GT1b mAb or control IgG and were following during 3 h by video time-lapse microscopy (acquiring images each 15 min) using a Spinning Disk Olympus DSU microscope, with a 60×/1.42 NA immersion objective.

### 2.7. Immunofluorescence

Dissociated DRGn cultures were fixed for 20 min in 4% paraformaldehyde, washed three times with PBS, and incubated for 1.5 h at room temperature with blocking solution (PBS, 5% normal horse serum, 0.02% Triton X-100 (Sigma)). Primary antibodies (anti-TUJ1 (Neuromics) diluted 1:2000, anti-acetyl-α-tubulin (Lys40 (Cell Signaling); diluted 1:500) or anti-tyrosine tubulin (clone TUB-1A2 (Sigma); diluted 1:1500) in blocking solution were added for 2 h at room temperature. Immunoreactivity was detected using anti-mouse Alexa Fluor® 488 conjugate (Invitrogen; diluted 1:500), biotinylated anti-rabbit IgG (diluted 1:500) and Streptavidin (Jackson Immunoresearch Laboratories, JIL); diluted 1:500) and Cy3-goat anti-mouse antibody (JIL; diluted 1:500) respectively and Acti-stain 555 Fluorescent Phalloidin (Cytoskeleton; diluted 1:250) for 1.5 h at room temperature. Tissues were mounted with Mowiol (Sigma-Aldrich).

### 2.8. Immunoblotting

Cultures of CHO-K1 cells (ATCC, Manassas, VA, USA) genetically modified to express gangliosides GM1 and GD1a (CHO-K1$^{GD1a+}$, described as clone 4 in Crespo et al., 2002 and kindly provided by Dr. J. Daniotti, Universidad Nacional de Córdoba) were transiently transfected with 1 μg/μl of rat Wt CRMP-2 vector backbone using

Lipofectamine 2000 (0.4 μl/well) in OptiMEM. Cells were grown for 24–48 h to allow cDNA expression and then treated with anti-GD1a/GT1b mAb (50 μg/ml) for different times and then harvested and homogenized in RIPA buffer containing 1% Triton X-100, 1% sodium deoxycholate, 0.1% SDS, 0.15 M NaCl, 0.05 M Tris–HCl, pH 7.2 containing protease inhibitor cocktail (Sigma, P8340). Homogenates were boiled for 5 min. After centrifugation (13,000 rpm, 10 min, 4 °C) the protein content of the supernatant was determined using the DC assay (Bio-Rad Life Science). Cell homogenates were diluted in Laemmli buffer and separated on a 10% SDS-polyacrylamide gel (100 μg/lane). Immunoblotting was performed with polyclonal IgG rabbit anti-CRMP2 (Thr-555) antibody diluted 1:100 (ECM Biosciences). To ensure that equal amounts of protein were loaded, tubulin immunoreactivity was determined under the same conditions as described, using a monoclonal anti-α-tubulin Ab (clone 12G10) diluted 1:1000 and horseradish peroxidase-conjugated goat anti-mouse IgG diluted 1:5000 (JIL). Membranes were developed using enhanced chemiluminescence. mAb 12G10 generated by investigators Frankel and Nelsen was obtained from the Developmental Studies Hybridoma Bank developed under the auspices of the NICHD and maintained by The University of Iowa, Department of Biology, Iowa City, IA, USA.

### 2.9. Analysis of GC morphology

The lamellipodia area was defined as $Area_{lamellipodia} = Area_{F\text{-}actin} - Area_{beta\text{-}III\text{-}tubulin}$ (Laishram et al., 2009); the tubulin ratio was defined as acetylated tubulin area/tyrosinated tubulin area (Witte et al., 2008). Filopodial length was measured from the base to their tip and following all branches. The GC surface area and the length of filopodia were measured with Fiji software (an open-source platform); (n = 40–60 GCs per group).

### 2.10. Neurite outgrowth assay

DRGn electroporated with Wt CRMP-2 or CRMP-2 T555A were cultured for 24 h to allow appropriate expression of plasmids. Cells were then replated and cultured in the presence of anti GD1a/GT1b mAb or IgG control (50 μg/ml). After 24 h cells were fixed for 20 min in 4% paraformaldehyde and stained with an anti-FLAG antibody (1:500; Sigma-Aldrich) and developed with Alexa Fluor® 488 conjugated secondary antibody (1:500; Molecular Probes). Images were acquired using a fluorescence microscope (Zeiss) and using 20×/0.8 NA air objective and analyzed with Fiji software. The length of longest neurite of each neuron (≥one cell body diameter) was measured using ImageJ (n = 60–80 neurons per group).

### 2.11. Förster Resonance Energy Transfer (FRET)

Transient transfection with a FRET-based wild type RhoA biosensor vector (Addgene cat. #12150) was performed by electroporation of dissociated DRGs with the DNA (Pertz et al., 2006). Cells were cultured for 24 h (to allow DNA expression) and then replated (Saijilafu and Zhou, 2012) and treated at 5 h with 50 μg/ml mAb 1B7 for different times. Cells were then fixed with 4% paraformaldehyde/4% sucrose in PBS, mounted and FRET efficiencies estimated as described. Cells were visualized through a Spinning Disk Olympus DSU microscope, using a 60×/1.42 NA immersion objective. FRET map images reflecting RhoA activity in cells were calculated as described (Iacaruso et al., 2011; Palandri et al., 2015). Briefly, CFP and YFP images were acquired while exciting the donor. For emission ratio imaging, the following filter sets were used: 457 and 514 nm argon multiline laser of 40 mw Model 35-IMA 040-220 of CVI (Melles Griot). Fiji software was used to perform image analysis. All images were first shading-corrected and background-subtracted. The FRET image, because it had the largest signal-to-noise ratio and therefore provided the best distinction between the cell and the background, was thresholded to generate a binary mask with a value of zero outside the cell and a value of one inside the cell. After multiplication by this mask, the FRET image was divided by the CFP image to yield a ratio image reflecting RhoA activation throughout the GC.

### 2.12. In vivo DRG electroporation

8–10-week-old male C57/Bl6 mice were obtained from our Specific Pathogen Free animal facility. The mice were anesthetized with an intra-peritoneal injection of a mixture of ketamine (100 mg/kg) and xylazine (10 mg/kg). A dorsal hemilaminectomy was performed, and DRGs were surgically exposed and injected with 1 μg of vectors encoding either Wt CRMP-2 or CRMP-2 T555A together with the tubulin-GFP vector to allow visualization of electroporated neurons. DRGs were electroporated in the L4 or L5 DRGs using described parameters (Saijilafu et al., 2011). After electroporation, the wound was closed and the mice were allowed to recover before returning to their cages. All experiments involving animals were performed in accordance with the animal protocol approved by our Institutional Animal Care and Use Committee.

### 2.13. Sciatic nerve-crush model

A standardized mouse sciatic nerve-crush model was used (Lopez et al., 2010). Right sciatic nerves were crushed 35 mm rostral to the middle toe for 30 s with fine forceps one week after in vivo DRG electroporation. Separation of proximal and distal endoneurial contents indicated complete crush. Two groups of animals electroporated with either Wt CRMP-2 or CRMP-2 T555A vectors (3 mice each group) received a single intra-peritoneal (IP) injection of 1 mg of 1B7 mAb. Passive transfer studies with a non-related control IgG were omitted since it was previously documented that it does not interfere with the regenerating process (Lehmann et al., 2007; Lopez et al., 2010). On day 12 after nerve crush, sciatic nerves were harvested, postfixed with 4% paraformaldehyde at 4 °C and processed for immunofluorescence analysis. The images of whole mount nerves were acquired with an Olympus FV1000 confocal microscope equipped with a CCD camera controlled by Fluoview software (Olympus.). For in vivo axon regeneration, every identifiable GFP-labeled axon in the sciatic nerve 100 μm proximal to the lesion site and 100, 200 and 300 μm distal to the lesion was manually traced to measure the axon length. Axon regeneration was quantified as the ratio of number of axons proximal to the lesion/number of axons distal to the lesion.

### 2.14. Statistical analyses

Data analysis was performed using standard statistical packages (InfoStat System). All values are shown as the mean ± SEM of at least three independent experiments. Student's-test or one-way analysis of variance (ANOVA) followed by LSD-Fisher *post hoc* test was used to assess differences. Background fluorescence was subtracted from the raw images, which were then overlaid as a stack.

## 3. Results

### 3.1. Anti-GD1a/GT1b mAb treatment alters GC cytoskeleton from primary dissociated DRGn cultures

We first examined the effect of mAb 1B7 in GC's cytoskeleton from primary dissociated postnatal-DRGn. Treatments included the addition of 50 μg/ml of GD1a/GT1b mAb at 1 h and 5 h after plating the cells to study its effect on initial neurite outgrowth and extension. Cultures were fixed 3 h later and components of the actin and MT cytoskeleton stained with phalloidin and with a mAb against class III β-tubulin (Clone TUJ-1), respectively. Treatment with mAb 1B7 5 h after plating

results in a significant reduction of GC lamellipodia (a complete collapse was observed in many cells) and reduced filopodial length when compared to IgG-treated control cultures (Fig. 1A–D, G and H). In addition, mAb 1B7-treated neurons showed GCs with F-actin aggregates at the central core. This treatment also altered tubulin signal, where TUJ-1 immunolabeling appeared more intense and diffuse along the central core of the GCs (Fig. 1A and B). More importantly, further analysis of MT organization in mAb 1B7-treated GCs showed an increased

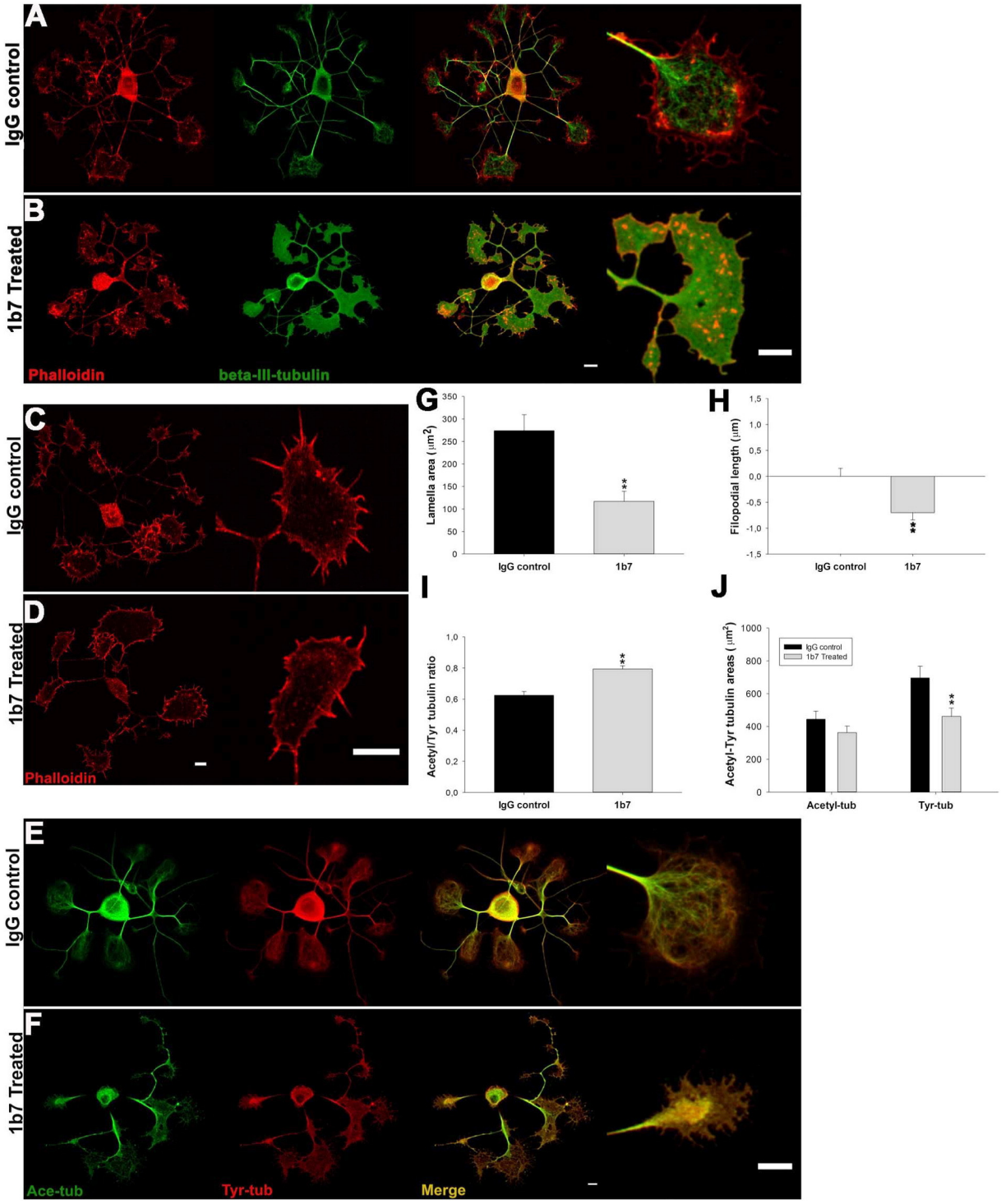


**Fig. 1.** Treatment of dissociated DRG neurons (DRGn) with mAb anti-GD1a/GT1b alters actin and tubulin cytoskeleton in growing GC. The effect of mAb 1B7 on neurite growth was tested in a neurite outgrowth paradigm. DRGn were treated 1 h after plating with 50 μg/ml of IgG control (A, C and E) or mAb 1B7 (B, D and F). After 5 h, cultures were fixed and stained with phalloidin to visualize F-actin (A, B, C and D), or antibodies against class III β-tubulin to visualize tubulin network (TUJ-1, A and B) as well as acetylated and tyrosinated tubulin to visualize stable and dynamics MTs respectively (E and F). Representative fluorescence micrographs of each experimental condition are depicted. Quantification of filopodial length (G, n: 63 GCs), lamella area (H, n: 63 GCs), ratio of acetylated/tyrosinated tubulin (I, n: 84 GCs) and acetylated/tyrosinated MT areas (J, n: 84 GCs) was achieved by image analysis (ImageJ). Symbols indicate statistical comparison with control. **$p < 0.01$ Student's t test, two tailed. Scale bar: 10 μm. Error bars indicate SEM.

acetylated (stable)/tyrosinated (dynamic) MT ratio associated with a significant decrease in the Tyr-tubulin area (Fig. 1E, F, I and J). Similar alterations in cytoskeleton organization were observed when DRGn were treated with mAb 1B7 1 h after plating (data not shown).

### 3.2. Temporal dissociation of mAb 1B7-induced GC actin and tubulin alterations

Temporal analysis of 1B7 mAb-induced alterations in GC's cytoskeleton was further evaluated using time-lapse video microscopy. To this end, DRGn were nucleofected with green fluorescent protein (GFP)-tagged α-tubulin (tubulin-GFP) and mCherry-tagged Lifeact (Lifeact-mCherry) and GC morphology and cytoskeletal organization evaluated by live imaging. Control cultures included pre-treatment for 1 h with 10 mU/ml of *V. cholerae* sialidase to hydrolyze sialic acid residues and eliminate anti-ganglioside Ab binding. Treatment with mAb 1B7 induced a progressive collapse of actin lamellipodia noticeable at 30 min, and reaching its maximum effect at about 90 min (Fig. 2B and C); a reduction of filopodial length was observed at about 60 min, where it reached its plateau. The effects of 1B7 mAb treatment on tubulin cytoskeleton were also detected 60 min after treatment; they were characterized by a progressive retraction of tubulin-GFP area when measured up to 120 min after Ab treatment (Fig. 2B and E). Overall anti-GD1a/GT1b mAb treatment results in temporal dissociation of morphological alterations at GCs from DRGn.

### 3.3. Anti-GD1a/GT1b mAb induces morphological alterations in GCs via RhoA/ROCK-dependent and independent pathways

It was previously reported that GD1a/GT1b mAb inhibited neurite outgrowth extension of DRGn via activation of RhoA/ROCK signaling pathways (Zhang et al., 2011). Since this mAb induces temporally dissociated morphological alterations in GCs from DRGn, we hypothesized that this could be reflecting the activation of different signaling pathways. To further analyze this question, DRGn were electroporated with a vector containing a FRET-based RhoA biosensor and cultured for 24 h to allow its appropriate expression; then cells were mechanically detached and re-plated for 5 h. RhoA activity was later quantified on GCs from DRG cultures treated with 1B7 mAb (50 μg/ml) for different time periods up to 90 min. We observed a significant transient increase in RhoA activity in GCs 30 min after mAb 1B7 treatment that parallels the collapse of the actin lamellipodia but precedes filopodial retraction and reduction of tubulin area (Fig. 3A and B). These results were further analyzed using a cell permeable version of exoenzyme C3 transferase, TAT-C3, a specific pharmacological inhibitor of Rho GTPases. Treatment of DRGn with 1 μg/ml of TAT-C3 1 h prior to the addition of 1B7 mAb failed to prevent the reduction of lamellipodia area but succeed in

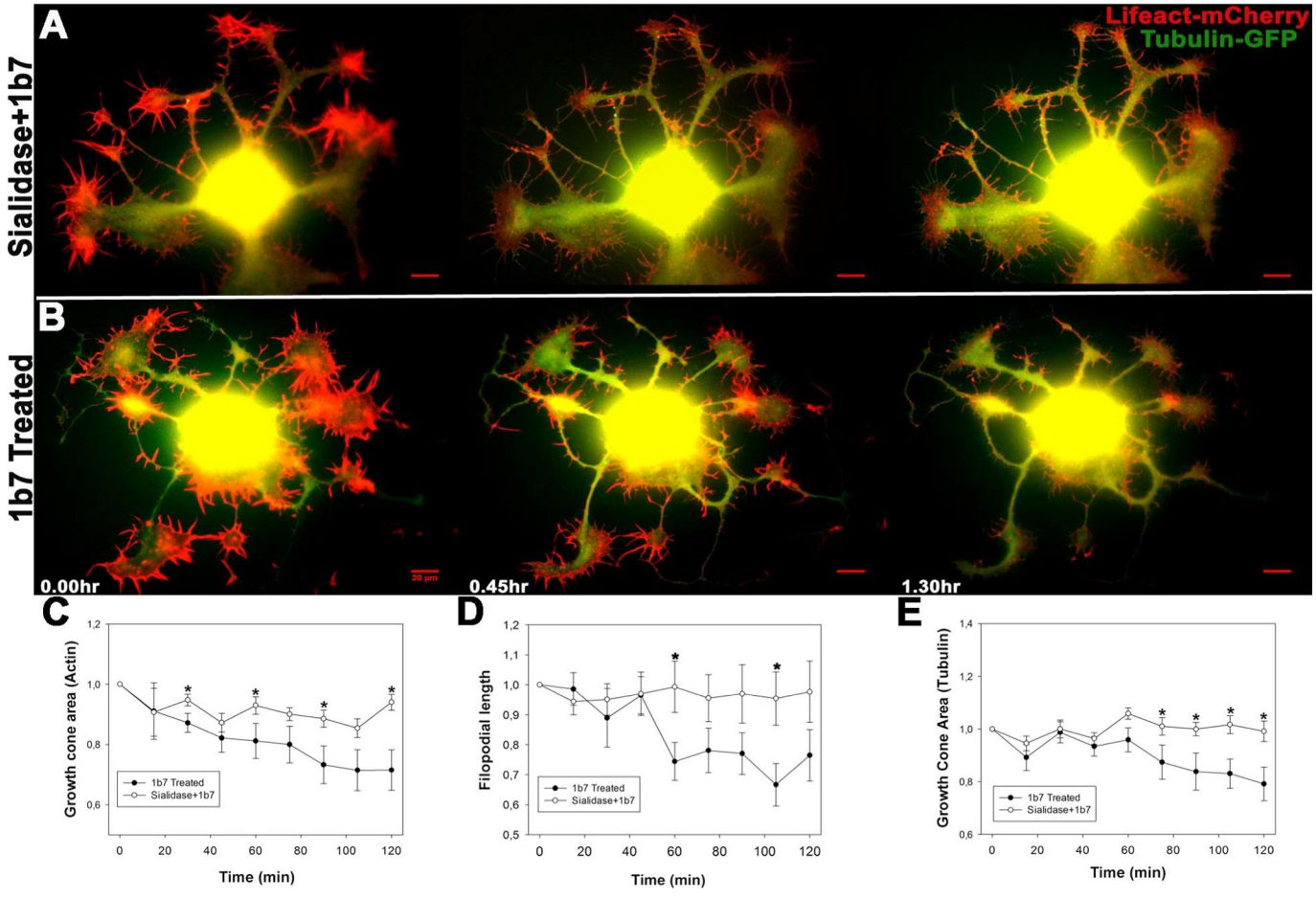


**Fig. 2.** Time-course study of mAb anti-GD1a/GT1b-induced changes in cytoskeleton. The effect of mAb 1B7 on neurite growth was tested in a paradigm of neurite extension. DRGn were plated and 1 h later nucleofected with life-actin (red) and tubulin-GFP (green). Then DRGn were treated 6 h after plating with 50 μg/ml of mAb 1B7 and time-lapse recorded every 15 min for 90 min. As control, DRGn were pre-treated with 10 mU/ml of sialidase to remove target gangliosides. A and B: Representative fluorescence micrographs of each experimental condition (0, 45 and 90 min are shown). Quantification of relative GC actin area (C, n: 26 GC), GC tubulin area (D, n: 27 GCs), and filopodial length (E, n: 26 GCs) was achieved by image analysis and normalized with respect to time 0 (T0) (ImageJ). Symbols indicate statistical comparison between sialidase-treated and untreated cultures. *$p < 0.05$ Student's t test, two tailed. Scale bar: 20 μm. Error bars indicate SEM.

preventing the shrinking of filopodia (in fact increased filopodial length) (Fig. 3E, G, J and L) and loss of dynamic MTs at the GCs, therefore preserving the acetylated/tyrosinated MT ratio (Fig. 4C and E). Similar results were observed when treating DRGn with two different concentrations (2 and 10 μM) of Y-27632, a specific inhibitor of Rho-associated kinases (ROCK, only results of cultures treated with 10 μM of Y-27,632 are shown). Pre-treatment of DRGn with Y-27632 failed to block the collapse of lamellipodia induced by GD1a/GT1b mAb while preserving GC's MT dynamics (similar ratio of acetylated/tyrosinated MTs to IgG-treated control, Fig. 4D and E) and promoting significant extension of filopodia (Fig. 3F, G, K and L). Altogether these results suggest that 1B7 mAb induces morphological alteration in GCs via RhoA/ROCK-dependent and independent pathways.

### *3.4. Anti-GD1a/GT1b mAb treatment inhibits neurite outgrowth via ROCK-dependent phosphorylation/inactivation of Collapsin Response Mediator Protein 2 at Thr555*

We next studied the downstream target of RhoA/ROCK pathway involved in the inhibitory effect of 1B7 mAb on GC morphology and cytoskeletal organization. It was previously found that myelin-associated glycoprotein (MAG), a major myelin-derived inhibitor of axon regeneration, inhibits neurite outgrowth of cerebellar granule neurons via RhoA/ROCK-dependent pathways by targeting its downstream target Collapsin Response Mediator Protein 2 (CRMP-2) (Mimura et al., 2006). Since the inhibitory action of MAG on these cells largely relies on binding to gangliosides GD1a and/or GT1b, we hypothesized that 1B7 mAb could alter GC organization and inhibit neurite length by a similar signaling mechanism (Mehta et al., 2007; Venkatesh et al., 2007). We first studied by immunofluorescence whether mAb 1B7 can induce a ROCK-dependent phosphorylation/inactivation of CRMP-2 at Thr555. DRGn cultures treated for 30 min with 50 μg/ml of 1B 7mAb showed an increased phosphorylation of CRMP-2 at Thr555 along the axon shaft compared to IgG-treated control cultures (Fig. 5A, B and D). These results were further confirmed by western blot analysis in homogenates of a stable CHO cell line displaying high ganglioside GD1a expression (CHO-K1$^{GD1a+}$) and further transfected with a vector containing the WT CRMP-2 sequence. Treatment of cell cultures with 50 μg/ml of 1B7 mAb induced significantly increased phosphorylation of CRMP-2 at Thr555 at 30 min but not at 60 min post-treatment (Fig. 5C).

Then we analyzed the effect of 1B7 mAb on neurite outgrowth in DRGn expressing a mutant form of CRMP-2, in which Thr555 had been replaced by a nonphosphorylatable residue (alanine, CRMP-2T555A), rendering the protein resistant to the regulatory action of ROCK. To this end, DRGn were electroporated with FLAG-tagged Wt CRMP-2 or CRMP-2-T555A constructs and 1 h after plating treated with 1B7 mAb (50 μg/ml) for an additional 23 h. DRGn transfected with Wt CRMP-2 and treated with 1B7 mAb showed an inhibition of 36% in neurite length with respect to control IgG-treated cultures. On the contrary, the inhibitory action of 1B7 mAb on neurite length was significantly reversed on DRGn overexpressing the mutant CRMP-2-T555A construct (17% difference respect to control cultures, $p \geq 0.05$; Fig. 5E–I). Taking together these results identified CRMP-2 as a downstream target of RhoA/ROCK signaling pathways mediating neurite growth-inhibitory activity of anti-ganglioside Ab.

### *3.5. In vivo DRG electroporation of a mutant form of CRMP-2 at the ROCK-dependent phosphorylation site (CRMP-2 T555A) overcame the inhibitory effect of anti-ganglioside mAb in an animal model of axon regeneration*

As a proof of principle, the role of CRMP-2 as a mediator of the inhibitory effect of anti-ganglioside Abs on axon regeneration downstream of RhoA/ROCK signaling pathways was further confirmed in an established animal model of axon regeneration. FLAG-tagged Wt CRMP-2 or CRMP-2-T555A constructs were co-electroporated in combination with a tubulin-GFP construct in L4–L5 DRGs from 3 month old C57Bl/6 mice and one week later a crush was performed at the mid-thigh sciatic level. Then mice were treated with a single dose of 1 mg/ml of 1B7 mAb 24 h after the nerve lesion and axon regeneration studied 12 days later in sciatic nerve segments distal to the crush site. Axon regeneration was assessed by counting the number of axons in the first 300 μm distal to the crush site. Expression of Wt CRMP-2 or CRMP-2-T555A constructs did not affect axon regeneration in mice without Ab treatment (data not shown). We observed that IP treatment with 1B7 mAb induced a strong inhibition of axon regeneration in mice electroporated with Wt CRMP-2 construct (Fig. 6A, C, D). On the contrary, axons from DRGn expressing CRMP-2-T555A display a robust regenerative capacity despite the presence of 1B7 mAb (Fig. 6B, E, F). Quantification of axon regeneration (ratio of the number of axons post-crush respect to the number of axons pre-crush) indicates that more than 70% of axons from DRGn expressing CRMP-2-T555A regenerate to 300 μm post-crush whereas only ~20% of axons expressing Wt CRMP-2 reached this distance (Fig. 6G). These findings further confirm the in vivo role of CRMP-2 as a downstream effector of RhoA/ROCK signaling pathways mediating the inhibitory effect of anti-ganglioside antibodies on nerve regeneration.

## 4. Discussion

Several reports have linked the presence of high titers of anti-Gg Abs with delayed recovery/poor prognosis in GBS (Carpo et al., 1999; Press et al., 2001; Ilyas et al., 1992; Gregson et al., 1993; Simone et al., 1993; Jacobs et al., 1996; Bech et al., 1997; Kuwabara et al., 1998; Annunziata et al., 2003; Koga et al., 2003). In most cases, failure to recover is associated with halted/deficient axon regeneration (Sheikh, 2011). Previous work identified that monoclonal and patient-derived anti-Gg Abs can act as inhibitory factors in an animal model of axon regeneration (Lehmann et al., 2007; Lopez et al., 2010). Further studies using primary neuronal cultures demonstrated that anti-Gg Abs can inhibit neurite outgrowth in DRGn by targeting gangliosides via activation of the small GTPase RhoA and its associated kinase (ROCK), a signaling pathway common to other well established inhibitors of axon regeneration (Zhang et al., 2011).

In the present study we performed a detailed characterization of the effects of anti-Gg Abs on the GC cytoskeletal organization of DRG cultured neurons. Our results demonstrate that in these neurons anti-Gg Abs: i) induce an early RhoA/ROCK-independent collapse of lamellipodia; ii) produce a RhoA/ROCK-dependent shrinking of filopodia; and iii) alter GC MT organization/and presumably dynamics via RhoA/ROCK-dependent phosphorylation of CRMP-2 at threonine 555. In accordance with this, our results also show that mAb 1B7 inhibits peripheral axon regeneration in an animal model system via phosphorylation/inactivation of CRMP-2 at threonine 555.

Myelin-derived inhibitors of axon regeneration (MIA) and guidance molecules described so far ultimately converge in the activation of a common signaling pathway via the small GTPase RhoA and its associated family of kinases (ROCK) to induce GC collapse. One such an example is myelin-associated glycoprotein (MAG), a sialic acid-binding immunoglobulin type-lectin that recognizes several axonal receptors including the complex gangliosides GD1a and GT1b (bearing the terminal NeuAcα3Galβ3GalNAc sugar structure) (Lopez, 2014). By targeting a multimeric receptor complex comprising ganglioside GT1b, Nogo receptor 1 (NgR1), LINGO-1 and the low affinity receptor for neurothrophins p75 (p75$^{NTR}$) acting as a transducer molecule, MAG can halt axon regeneration via activation of the downstream signaling pathway RhoA/ROCK; alternatively its orphan homolog TAJ/TROY can function as a traducer molecule in neurons lacking p75$^{NTR}$ expression (revised from Schnaar and Lopez, 2009). RhoA activation involves interaction of the intracellular domain of p75$^{NTR}$ with Rho-GDP dissociation inhibitor alpha (RhoGDIα), and further displacement of Rho-GDIα/RhoA complex (Yamashita and Tohyama, 2003).

Alternatively ganglioside-mediated activation of RhoA/ROCK signaling pathways by MAG can be achieved by yet unidentified transducer molecules; and this reflects in part the complexity of co-receptors and signaling molecules recruited by different axonal receptors in nerve cells (Mehta et al., 2007; Venkatesh et al., 2007). Similarly, mAb 1B7 can inhibit axon regeneration in primary DRGn cultures by targeting nerve gangliosides via activation of RhoA/ROCK signaling pathways in a $p75^{NTR}$-independent manner (Zhang et al., 2011). Also mAb 1B7 can

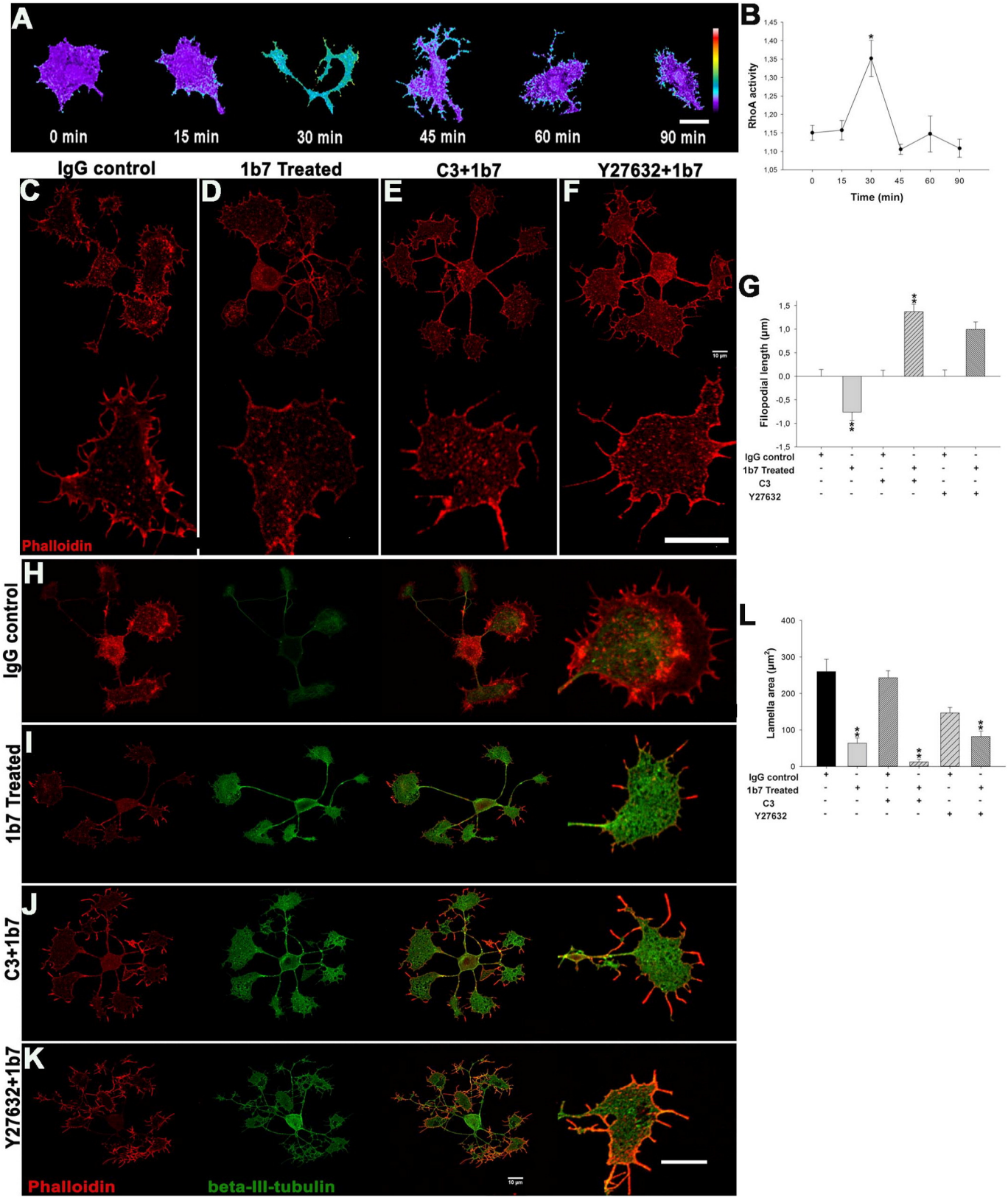

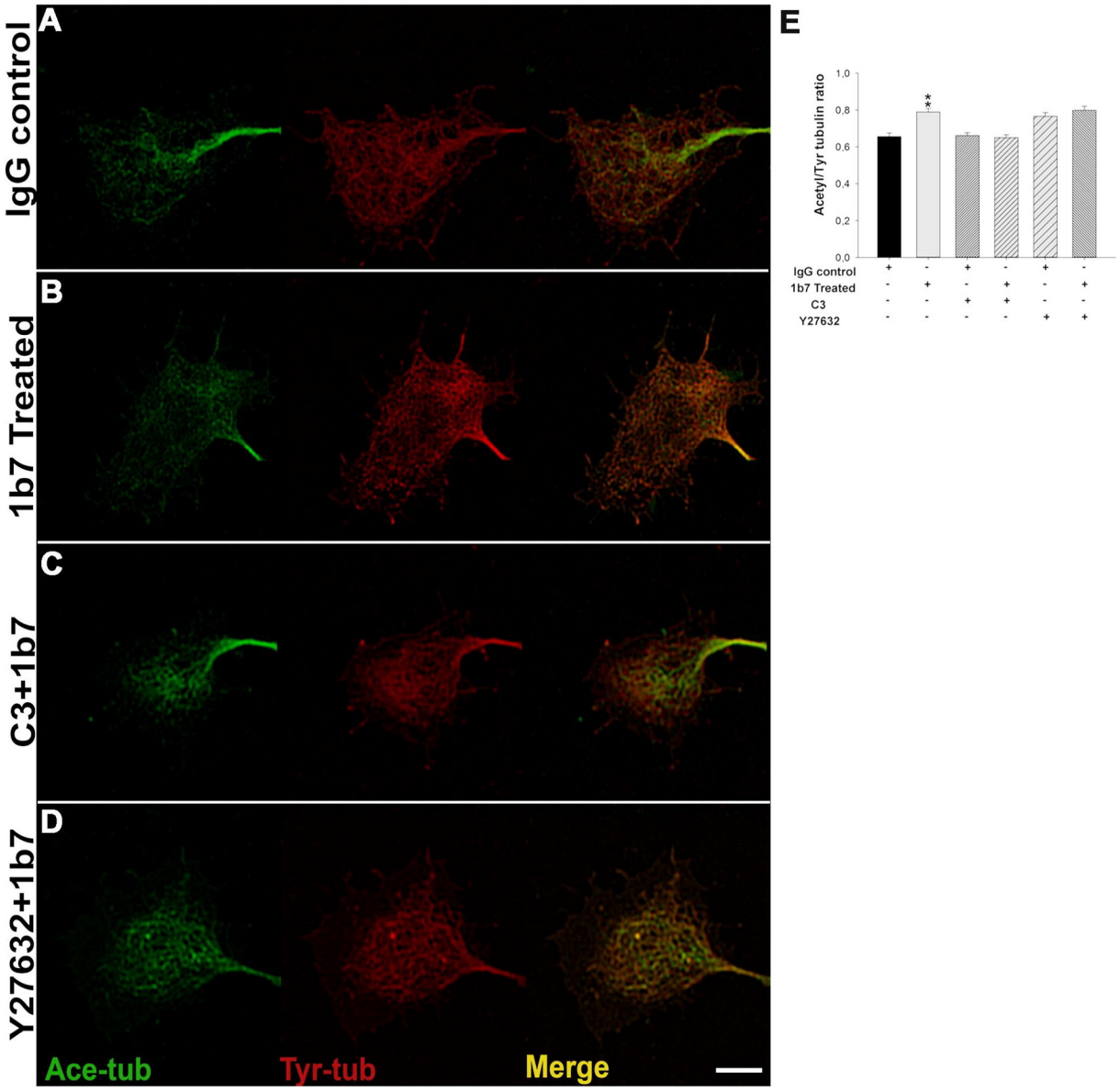


**Fig. 4.** Treatment with RhoA and ROCK inhibitors reverse the inhibitory effect of mAb anti-GD1a/GT1b on microtubule dynamics. DRGn were plated and 5 h later treated with 50 μg/ml of IgG control (A) or mAb 1B7 (B). In order to study the effect of C3 or Y-27632 in vitro, DRGn were cultures and treated 4 h after plating with 1 μg/ml of C3 transferase for 1 h (C) or 3 h after plating with 10 μM of Y-27632 for 2 h (D) and then cultures were treated with 50 μg/ml of mAb 1B7 or IgG control for 1.5 h. Cultures were fixed and stained with Abs against acetylated and tyrosinated tubulin to visualize stable and dynamics microtubules respectively (A–D). Representative fluorescence micrographs of each experimental condition are depicted. Scale bar: 10 μm. Quantification of acetylated/tyrosinated tubulin ratio (E, n: 361 GCs) was achieved by image analysis (ImageJ). Symbols indicate statistical comparison with their control culture.$^{**}p < 0.01$; ANOVA. LSD Fisher *post hoc test* n = 3. Error bars indicate SEM.

impair axon regeneration in $p75^{NTR}$ deficient mice, confirming the redundancy of $p75^{NTR}$ in this model. Although the role of TAJ/TROY cannot be yet excluded, the identity of the transducer molecule used by gangliosides still remains obscure. Despite being ubiquitous glycosphingolipids, gangliosides are highly concentrated in the nervous system. Expressed at the outer cell surface membrane, gangliosides interact with a great variety of membrane receptors modulating their activity (Lopez and Schnaar, 2009). However, Ab-mediated ganglioside crosslinking can also elicit the activation of membrane receptors without implying a direct interaction (Sonnino et al., 2013). This observation

**Fig. 3.** Treatment with RhoA and ROCK inhibitors has no effect on actin lamellipodia. A: Time course of RhoA activation in DRGn after treatment with mAb anti-GD1a/GT1b. DRGn were electroporated with a FRET-based RhoA biosensor 5 h before treatment with mAb 1B7 at 50 μg/ml. Images captured at different times (0, 15, 30, 45, 60 and 90 min) after mAb treatment illustrate the pseudo-color thermal map of RhoA activation on DRGn with a peak at 30 min after treatment (warm colors, high FRET activity; cold colors, low FRET activity). Representative fluorescence micrographs of each experimental time are depicted. B: Quantification of RhoA activation. Symbols indicate statistical comparison with control: $^{*}p < 0.05$ ANOVA-LSD Fisher *post hoc test* n = 4. C-F and H-K: DRGn were plated and 5 h later treated for 3 h with 50 μg/ml of IgG control (C and H) or mAb 1B7 (D and I). Representative fluorescence micrographs of each experimental condition are depicted. In order to study the effect of C3 or Y-27632 in vitro, DRGn were cultured and treated 4 h after plating with 1 μg/ml of C3 transferase for 1 h (E and J) or 3 h after plating with 10 μM of Y-27632 for 2 h (F and K) and then with 50 μg/ml of IgG control or mAb 1B7 for an additional 1.5. Cultures were fixed and stained with phalloidin to visualize F-actin (C–K) and antibodies against class III β-tubulin (TUJ-1, H–K) to visualize tubulin network. Quantification of relative filopodial length (G, n:456 GCs) and lamella area (L, n: 474 GCs) were achieved by image analysis (ImageJ). Symbols indicate statistical comparison with control. $^{**}p < 0.01$; ANOVA. LSD Fisher *post hoc test* n = 3. Error bars indicate SEM. Scale bars = 10 μm.

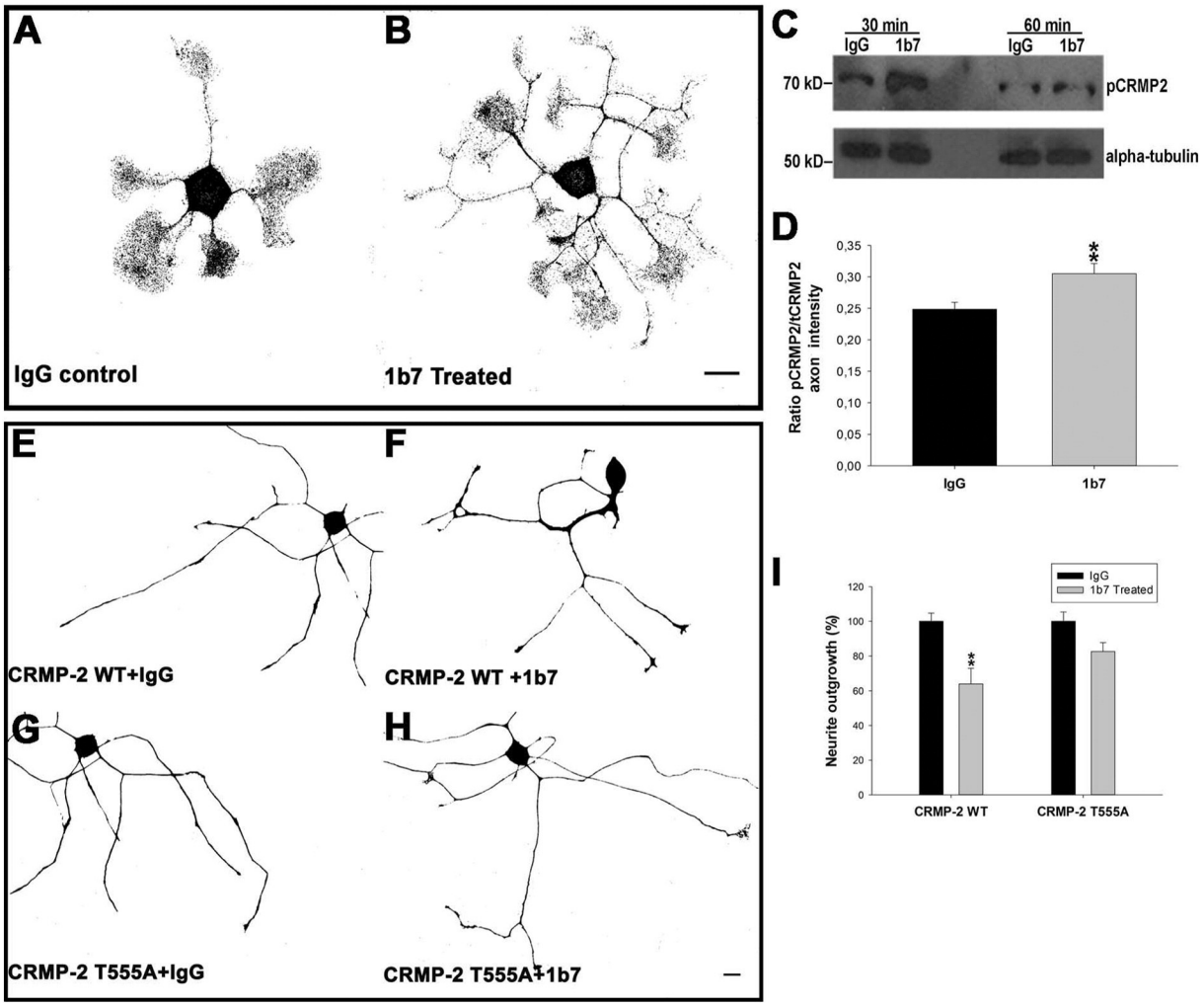


**Fig. 5.** A mutant form of CRMP-2 at the ROCK-dependent phosphorylation site (CRMP-2 T555A) reverses inhibition of neurite outgrowth produced by anti-GD1a/GT1b mAb. A–B: DRGn cultures were treated 5 h after plating with 50 μg/ml of mAb 1B7 or control IgG for 30 min. After fixation, DRGn were immunostained with Abs against pCRMP-2 T555 and tCRMP-2. Representative fluorescence micrographs are presented as reverse gray scale images to enhance clarity. D: Quantification of pCRMP-2/tCRMP-2 ratio by image analysis (ImageJ). Symbols indicate statistical comparison with 1B7-treated cultures. **, $p < 0.01$ Student's t test, two tailed, n: 70 GCs. C: CHO-K1$^{GD1a+}$ cells were transfected with Wt CRMP-2 and treated with 50 μg/ml mAb 1B7 or IgG at different times (30 and 60 min). Then cells were lysed and examined by western blot to check phosphorylation/inactivation of CRMP-2 at T555 induced by mAb 1B7. E–H: Dissociated DRG cultures were electroporated using Amaxa kit with Wt CRMP-2 and a mutant CRMP-2 in which threonine 555 has been replaced by a nonphosphorylatable residue (alanine, CRMP-2T555A), and treated 1 h after plating with 50 μg/ml of mAb 1B7 or control IgG for 24 h. Representative fluorescence micrographs of each experimental condition are depicted as reverse gray scale images to enhance clarity. I: Quantification of neurite outgrowth by image analysis (ImageJ). **, $p < 0.01$ Student's t test, two tailed, n: 273 GCs. Error bars indicate SEM. Scale bars = 20 μm.

and the lipid nature of gangliosides add more complexity to the current technical limitations to study their molecular interactions at the cell membrane.

Ultimately, inhibition of neurite outgrowth by MIA downstream of RhoA/ROCK pathway is achieved by modulating the activity of several effector molecules affecting cytoskeleton at GCs (Fujita and Yamashita, 2014). Two principal mechanisms modulating actin cytoskeleton has been described so far: collapsing of lamellipodia by stimulating myosin–actin contractility via a ROCK-dependent phosphorylation/activation of the regulatory light chain of myosin; and disruption of F-actin cytoskeleton via a ROCK/LIM Domain Kinase-1 (LIMK1)-dependent phosphorylation/inactivation of cofilin activity which in turn, triggers a chronic activation of Slingshot phosphatase resulting in high cofilin activity (Hsieh et al., 2006). Our findings on the molecular mechanisms associated with the inhibitory effect of anti-Gg Abs on axon regeneration highlight the presence of ROCK-dependent as well as independent mechanisms. Thus, Ab-mediated collapse of lamellipodia appeared as the first event triggered by anti-Gg antibodies at GCs, an event not prevented by inhibition of the RhoA/ROCK pathway. Alternatively neurite outgrowth inhibition can be achieved by activating LIMK1 via Rac1, another member of the Rho family of GTPases, in a p21-activated kinases 1 (PAK1)-dependent manner. This effect also involves the phosphorylation and subsequent dephosphorylation of cofilin at GCs; a mechanism resembling the effect of MIA (Aizawa et al., 2001). Current experiments have been conducted to answer whether modulation of Rac1 signaling pathway is involved in anti-ganglioside Ab-mediated lamellipodia collapse.

On the contrary, filopodial shrinkage and alterations in microtubule organization/dynamics follow RhoA activation at GCs and could be prevented by pharmacological inhibition of RhoA/ROCK pathway. Previous work described that ROCK-dependent modulation of microtubule network by MIA involves phosphorylation/inactivation of CRMP-2, affecting microtubule assembly (Mimura et al., 2006). Our data also demonstrates that Ab binding to cell surface gangliosides triggers a ROCK-dependent phosphorylation/inactivation of CRMP-2 at threonine 555, resulting in a critical step to inhibit neurite outgrowth extension in primary DRGn cultures. Moreover, in vivo electroporation in DRGn of a nonphosphorylatable mutant form of CRMP-2 at residue threonine 555 succeed to overcome anti-Gg Ab-mediated inhibition of axon regeneration, further emphasizing the role of RhoA/ROCK/CRMP-2 pathway on

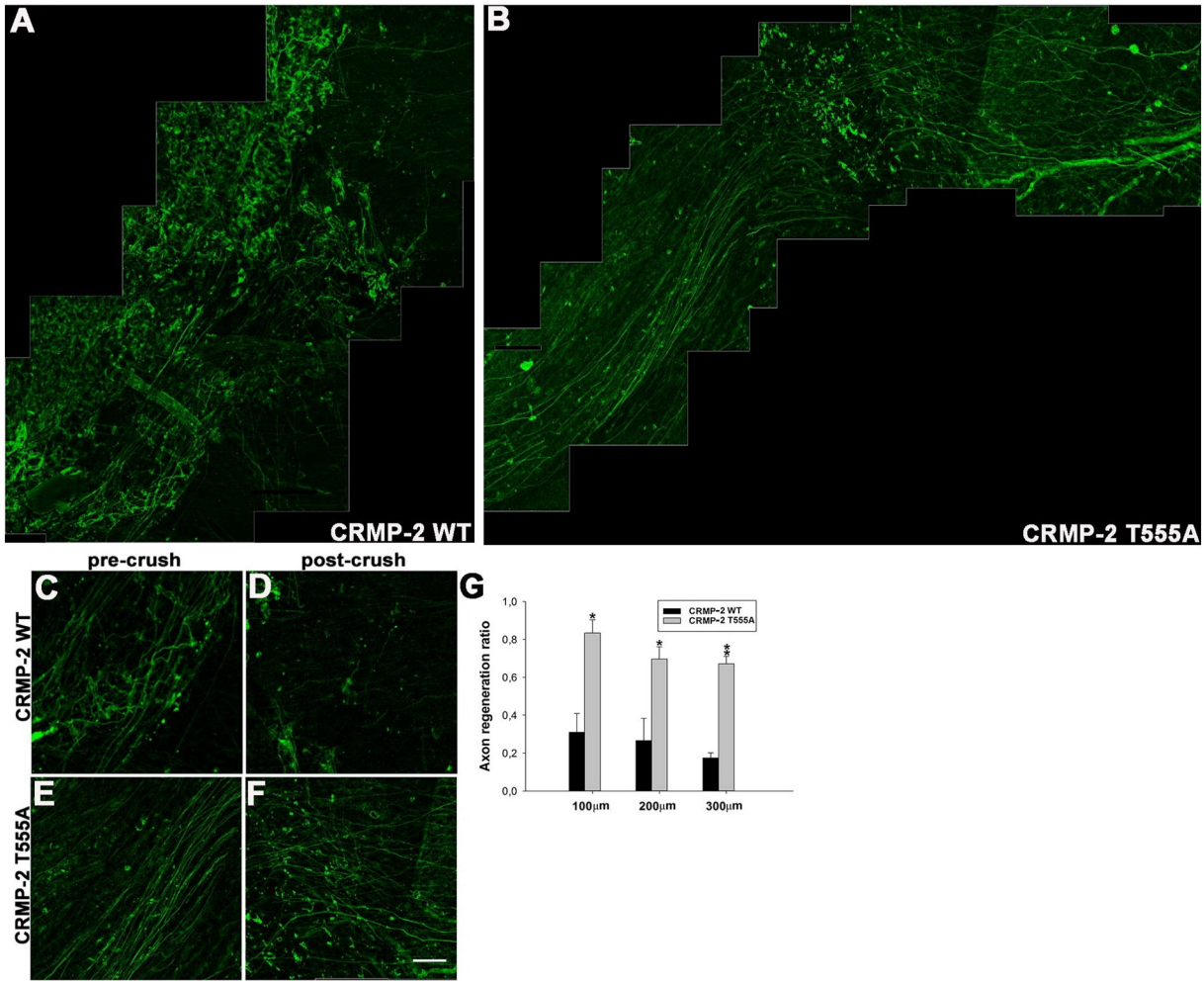


**Fig. 6.** In vivo electroporation of CRMP-2 T555A reverses axon regeneration inhibition produced by anti-GD1a/GT1b mAb. C57Bl/6 animals were coelectroporated with Wt CRMP-2 or T555A and tubulin-GFP in the L4–L6 DRG. They then underwent a sciatic nerve crush and i.p. injection with 1 mg/ml of mAb 1B7. Representative merged images of electroporated nerves with Wt CRMP-2 (A) and CRMP-2 T555A (B) in the area of the crush site. C–F: Enlarged images of axons from panels A and B showing regenerating GFP-labeled axons in the pre-crush zones (C and E) and post-crush zones (D and F). G: Quantification of axon regeneration (ratio of the number of axons distal to the crush site normalized to the number of axons proximal to the crush site) at 100, 200 and 300 µm distal to the crush site by image analysis (ImageJ). *$p < 0.05$ **$p < 0.01$ Student's t test, two tailed, n: 3 mice for each group. Error bars indicate SEM. Scale bars: 50 µm.

the inhibitory activity of anti-Gg antibodies on axon regeneration. In light of recent findings identifying the role of CRMP-2 in several neurodegenerative conditions as well as the effect of the atypical antidepressant and anxiolytic drug tianeptine, on increasing CRMP-2 expression and promoting neurite outgrowth on chick DRGn, it highlights CRMP-2 as a potential therapeutic target to promote axon regeneration in GBS (Hensley et al., 2011). Altogether our results identify a complex scenario where binding of anti-Gg Abs to nerve cells triggers the activation of multiple signaling pathways to halt axon regeneration and, at the same time, speak against a universal signaling pathway underlying GC collapse. An important question that need to be addressed is whether these signaling processes are connected or they just represent the activation of two independent pathways at different areas of the GCs. In this sense it was demonstrated that the microtubule-binding protein CRMP-4 forms a functional complex with RhoA modulating MTs and actin cytoskeleton at GCs in response to MIA (Khazaei et al., 2014; Alabed et al., 2007). Other evidences support a role for factors modulating Rho GTPases as a consequence of their release after MT depolymerization (Montenegro-Venegas et al., 2010; Conde et al., 2010; Conde et al., 2010; Chuang et al., 2005). We hypothesize that, independent of the initial signaling pathway responsible for RhoA-independent retraction of lamellipodia, the F-actin and MT depolymerization that follow this process release factors such as GEFs that subsequently converge in RhoA activation. If this is correct, then drugs promoting F-actin stability should prevent RhoA activation and overcome inhibition of neurite outgrow induced by crosslinking.

In contrast to many inhibitors of axon regeneration whose activity appears restricted to the glial scar surrounding the lesion site, anti-Gg Abs are soluble factors appearing as inhibitory cues all along the nerve regenerating process from the lesion site to the reinnervation of its target organ. It was recently proposed that axon regeneration in the central nervous system can be promoted by pharmacological stabilization of MTs, which counterbalance the MT retraction/instability triggered by inhibitors of axon regeneration (Hellal et al., 2011; Erturk et al., 2007). The potential therapeutic use of Y-27632, a specific inhibitor of ROCK, has been suggested by many pre-clinical studies and several phase II clinical trials, currently emerging as a successful treatment to promote axon regeneration in the central and peripheral nervous system (McKerracher et al., 2012; Forgione and Fehlings, 2014). Efficient target reinnervation is a key step toward clinical recovery, requiring an intact actin cytoskeleton able to guide GCs to their target organs. In peripheral nerves, axons are guided by factors released by Schwann cells and by their end-target organs (Scheib and Hoke, 2013). Therefore pharmacological treatments inducing assembly/stabilization of MTs, despite promoting axon extension, may result inadequate to support an accurate and efficient target reinnervation

due to their inability to restore lamellipodia at GCs in GBS patients with high titer of IgG anti-Gg antibodies.

The current work builds on previous observations showing the role of RhoA/ROCK signaling pathways on inhibition of axon regeneration induced by anti-Gg Abs by dissecting the molecular dynamics of GC cytoskeleton in response to anti-Gg Abs. Future work should define RhoA-independent pathway/s and effectors regulating actin cytoskeleton, which could have a pronounced effect toward the design of a successful therapy to guarantee an efficient target reinnervation.

## Conflict of interest

The authors declare no conflict of interest.

## Acknowledgments

This work was supported by grants from FONCyT-PICT-2010-2717 and GBS-CIDP International Foundation to P.H.H.L. P.H.H.L and A.C. are established scientists from CONICET. V.R.S and A.L.V. are PhD fellows from CONICET. J.W. and A.P. were supported with a PhD fellowship from CONICET. KAS is supported by the National Institute of Neurological Disorders and Stroke (NIH/NINDS; grant # NS42888, NS54962, NS087467. The authors thank Dr. Ronald Schnaar for critical reading of the manuscript and Dr. Gonzalo Quassollo for technical assistance with microscopy techniques.

## References

Aizawa, H., Wakatsuki, S., Ishii, A., Moriyama, K., Sasaki, Y., Ohashi, K., Sekine-Aizawa, Y., Sehara-Fujisawa, A., Mizuno, K., Goshima, Y., Yahara, I., 2001. Phosphorylation of cofilin by LIM-kinase is necessary for semaphorin 3A-induced growth cone collapse. Nat. Neurosci. 4, 367–373.

Alabed, Y.Z., Pool, M., Ong, T.S., Fournier, A.E., 2007. Identification of CRMP4 as a convergent regulator of axon outgrowth inhibition. J Neurosci 27, 1702–1711.

Annunziata, P., Figura, N., Galli, R., Mugnaini, F., Lenzi, C., 2003. Association of anti-GM1 antibodies but not of anti-cytomegalovirus, *Campylobacter jejuni* and *Helicobacter pylori* IgG, with a poor outcome in Guillain–Barre syndrome. J. Neurol. Sci. 213, 55–60.

Arimura, N., Inagaki, N., Chihara, K., Menager, C., Nakamura, N., Amano, M., Iwamatsu, A., Goshima, Y., Kaibuchi, K., 2000. Phosphorylation of collapsin response mediator protein-2 by Rho-kinase. Evidence for two separate signaling pathways for growth cone collapse. J. Biol. Chem. 275, 23973–23980.

Arimura, N., Menager, C., Kawano, Y., Yoshimura, T., Kawabata, S., Hattori, A., Fukata, Y., Amano, M., Goshima, Y., Inagaki, M., Morone, N., Usukura, J., Kaibuchi, K., 2005. Phosphorylation by Rho kinase regulates CRMP-2 activity in growth cones. Mol. Cell. Biol. 25, 9973–9984.

Bech, E., Orntoft, T.F., Andersen, L.P., Skinhoj, P., Jakobsen, J., 1997. IgM anti-GM1 antibodies in the Guillain–Barre syndrome: a serological predictor of the clinical course. J. Neuroimmunol. 72, 59–66.

Bradke, F., Fawcett, J.W., Spira, M.E., 2012. Assembly of a new growth cone after axotomy: the precursor to axon regeneration. Nat. Rev. Neurosci. 13, 183–193.

Brown, W.F., Feasby, T.E., 1984. Conduction block and denervation in Guillain–Barre polyneuropathy. Brain 107 (Pt 1), 219–239.

Brown, M., Jacobs, T., Eickholt, B., Ferrari, G., Teo, M., Monfries, C., Qi, R.Z., Leung, T., Lim, L., Hall, C., 2004. Alpha2-chimaerin, cyclin-dependent kinase 5/p35, and its target collapsin response mediator protein-2 are essential components in semaphorin 3A-induced growth-cone collapse. J. Neurosci. 24, 8994–9004.

Carpo, M., Pedotti, R., Allaria, S., Lolli, F., Mata, S., Cavaletti, G., Protti, A., Pomati, S., Scarlato, G., Nobile-Orazio, E., 1999. Clinical presentation and outcome of Guillain–Barre and related syndromes in relation to anti-ganglioside antibodies. J. Neurol. Sci. 168, 78–84.

Chen, K., Ye, Y., Ji, Z., Tan, M., Li, S., Zhang, J., Guo, G., Lin, H., 2014. Katanin p60 promotes neurite growth and collateral formation in the hippocampus. Int. J. Clin. Exp. Med. 7, 2463–2470.

Chuang, J.Z., Yeh, T.Y., Bollati, F., Conde, C., Canavosio, F., Caceres, A., Sung, C.H., 2005. The dynein light chain Tctex-1 has a dynein-independent role in actin remodeling during neurite outgrowth. Dev. Cell 9, 75–86.

Conde, C., Arias, C., Robin, M., Li, A., Saito, M., Chuang, J.Z., Nairn, A.C., Sung, C.H., Caceres, A., 2010. Evidence for the involvement of Lfc and Tctex-1 in axon formation. J. Neurosci. 30, 6793–6800.

Crespo, P.M., Zurita, A.R., Daniotti, J.L., 2002. Effect of gangliosides on the distribution of a glycosylphosphatidylinositol-anchored protein in plasma membrane from Chinese hamster ovary-K1 cells. J. Biol. Chem. 277, 44731–44739.

Erturk, A., Hellal, F., Enes, J., Bradke, F., 2007. Disorganized microtubules underlie the formation of retraction bulbs and the failure of axonal regeneration. J. Neurosci. 27, 9169–9180.

Forgione, N., Fehlings, M.G., 2014. Rho-ROCK inhibition in the treatment of spinal cord injury. World Neurosurg. 82, e535–e539.

Fujita, Y., Yamashita, T., 2014. Axon growth inhibition by RhoA/ROCK in the central nervous system. Front. Neurosci. 8, 338.

Gong, Y., Tagawa, Y., Lunn, M.P., Laroy, W., Heffer-Lauc, M., Li, C.Y., Griffin, J.W., Schnaar, R.L., Sheikh, K.A., 2002. Localization of major gangliosides in the PNS: implications for immune neuropathies. Brain 125, 2491–2506.

Gordon-Weeks, P.R., 1987. The cytoskeletons of isolated, neuronal growth cones. Neuroscience 21, 977–989.

Gregson, N.A., Koblar, S., Hughes, R.A., 1993. Antibodies to gangliosides in Guillain–Barre syndrome: specificity and relationship to clinical features. Q. J. Med. 86, 111–117.

Hall, C., Brown, M., Jacobs, T., Ferrari, G., Cann, N., Teo, M., Monfries, C., Lim, L., 2001. Collapsin response mediator protein switches RhoA and Rac1 morphology in N1E-115 neuroblastoma cells and is regulated by Rho kinase. J. Biol. Chem. 276, 43482–43486.

Hellal, F., Hurtado, A., Ruschel, J., Flynn, K.C., Laskowski, C.J., Umlauf, M., Kapitein, L.C., Strikis, D., Lemmon, V., Bixby, J., Hoogenraad, C.C., Bradke, F., 2011. Microtubule stabilization reduces scarring and causes axon regeneration after spinal cord injury. Science 331, 928–931.

Hensley, K., Venkova, K., Christov, A., Gunning, W., Park, J., 2011. Collapsin response mediator protein-2: an emerging pathologic feature and therapeutic target for neurodisease indications. Mol. Neurobiol. 43, 180–191.

Hsieh, S.H., Ferraro, G.B., Fournier, A.E., 2006. Myelin-associated inhibitors regulate cofilin phosphorylation and neuronal inhibition through LIM kinase and slingshot phosphatase. J. Neurosci. 26, 1006–1015.

Iacaruso, M.F., Galli, S., Marti, M., Villalta, J.I., Estrin, D.A., Jares-Erijman, E.A., Pietrasanta, L.I., 2011. Structural model for p75(NTR)-TrkA intracellular domain interaction: a combined FRET and bioinformatics study. J. Mol. Biol. 414, 681–698.

Ilyas, A.A., Mithen, F.A., Dalakas, M.C., Chen, Z.W., Cook, S.D., 1992. Antibodies to acidic glycolipids in Guillain–Barre syndrome and chronic inflammatory demyelinating polyneuropathy. J. Neurol. Sci. 107, 111–121.

Jacobs, B.C., van Doorn, P.A., Schmitz, P.I., Tio-Gillen, A.P., Herbrink, P., Visser, L.H., Hooijkass, H., van der Meche, F.G., 1996. Campylobacter jejuni infections and anti-GM1 antibodies in Guillain–Barre syndrome. Ann. Neurol. 40, 181–187.

Khazaei, M.R., Girouard, M.P., Alchini, R., Ong, T.S., Shimada, T., Bechstedt, S., Cowan, M., Guillet, D., Wiseman, P.W., Brouhard, G., Cloutier, J.F., Fournier, A.E., 2014. Collapsin response mediator protein 4 regulates growth cone dynamics through the actin and microtubule cytoskeleton. J. Biol. Chem. 289, 30133–30143.

Koga, M., Yuki, N., Hirata, K., Morimatsu, M., Mori, M., Kuwabara, S., 2003. Anti-GM1 antibody IgG subclass: a clinical recovery predictor in Guillain–Barre syndrome. Neurology 60, 1514–1518.

Kuwabara, S., Asahina, M., Koga, M., Mori, M., Yuki, N., Hattori, T., 1998. Two patterns of clinical recovery in Guillain–Barre syndrome with IgG anti-GM1 antibody. Neurology 51, 1656–1660.

Laishram, J., Kondra, S., Avossa, D., Migliorini, E., Lazzarino, M., Torre, V., 2009. A morphological analysis of growth cones of DRG neurons combining atomic force and confocal microscopy. J. Struct. Biol. 168, 366–377.

Lehmann, H.C., Lopez, P.H., Zhang, G., Ngyuen, T., Zhang, J., Kieseier, B.C., Mori, S., Sheikh, K.A., 2007. Passive immunization with anti-ganglioside antibodies directly inhibits axon regeneration in an animal model. J. Neurosci. 27, 27–34.

Lopez, P.H., 2014. Role of myelin-associated glycoprotein (siglec-4a) in the nervous system. Adv. Neurobiol. 9, 245–262.

Lopez, P.H., Schnaar, R.L., 2009. Gangliosides in cell recognition and membrane protein regulation. Curr. Opin. Struct. Biol. 19, 549–557.

Lopez, P.H., Zhang, G., Zhang, J., Lehmann, H.C., Griffin, J.W., Schnaar, R.L., Sheikh, K.A., 2010. Passive transfer of IgG anti-GM1 antibodies impairs peripheral nerve repair. J. Neurosci. 30, 9533–9541.

Lunn, M.P., Johnson, L.A., Fromholt, S.E., Itonori, S., Huang, J., Vyas, A.A., Hildreth, J.E., Griffin, J.W., Schnaar, R.L., Sheikh, K.A., 2000. High-affinity anti-ganglioside IgG antibodies raised in complex ganglioside knockout mice: reexamination of GD1a immunolocalization. J. Neurochem. 75, 404–412.

McKerracher, L., Ferraro, G.B., Fournier, A.E., 2012. Rho signaling and axon regeneration. Int. Rev. Neurobiol. 105, 117–140.

Mehta, N.R., Lopez, P.H., Vyas, A.A., Schnaar, R.L., 2007. Gangliosides and Nogo receptors independently mediate myelin-associated glycoprotein inhibition of neurite outgrowth in different nerve cells. J. Biol. Chem. 282, 27875–27886.

Mimura, F., Yamagishi, S., Arimura, N., Fujitani, M., Kubo, T., Kaibuchi, K., Yamashita, T., 2006. Myelin-associated glycoprotein inhibits microtubule assembly by a Rho-kinase-dependent mechanism. J. Biol. Chem. 281, 15970–15979.

Montenegro-Venegas, C., Tortosa, E., Rosso, S., Peretti, D., Bollati, F., Bisbal, M., Jausoro, I., Avila, J., Caceres, A., Gonzalez-Billault, C., 2010. MAP1B regulates axonal development by modulating Rho-GTPase Rac1 activity. Mol. Biol. Cell 21, 3518–3528.

Palandri, A., Salvador, V.R., Wojnacki, J., Vivinetto, A.L., Schnaar, R.L., Lopez, P.H., 2015. Myelin-associated glycoprotein modulates apoptosis of motoneurons during early postnatal development via NgR/p75(NTR) receptor-mediated activation of RhoA signaling pathways. Cell Death Dis. 6, e1876.

Pertz, O., Hodgson, L., Klemke, R.L., Hahn, K.M., 2006. Spatiotemporal dynamics of RhoA activity in migrating cells. Nature 440, 1069–1072.

Press, R., Mata, S., Lolli, F., Zhu, J., Andersson, T., Link, H., 2001. Temporal profile of anti-ganglioside antibodies and their relation to clinical parameters and treatment in Guillain–Barre syndrome. J. Neurol. Sci. 190, 41–47.

Saijilafu, Zhou, F.Q., 2012. Genetic study of axon regeneration with cultured adult dorsal root ganglion neurons. J. Vis. Exp.

Saijilafu, Hur, E.M., Zhou, F.Q., 2011. Genetic dissection of axon regeneration via in vivo electroporation of adult mouse sensory neurons. Nat. Commun. 2, 543.

Scheib, J., Hoke, A., 2013. Advances in peripheral nerve regeneration. Nat. Rev. Neurol. 9, 668–676.

Schnaar, R.L., Lopez, P.H., 2009. Myelin-associated glycoprotein and its axonal receptors. J. Neurosci. Res. 87, 3267–3276.
Sheikh, K.A., 2011. Autoantobodies activate small GTPase RhoA to modulate neurite outgrowth. Small GTPases 2, 233–238.
Simone, I.L., Annunziata, P., Maimone, D., Liguori, M., Leante, R., Livrea, P., 1993. Serum and CSF anti-GM1 antibodies in patients with Guillain–Barre syndrome and chronic inflammatory demyelinating polyneuropathy. J. Neurol. Sci. 114, 49–55.
Sonnino, S., Mauri, L., Ciampa, M.G., Prinetti, A., 2013. Gangliosides as regulators of cell signaling: ganglioside-protein interactions or ganglioside-driven membrane organization? J. Neurochem. 124, 432–435.
Tan, M., Cha, C., Ye, Y., Zhang, J., Li, S., Wu, F., Gong, S., Guo, G., 2015. CRMP4 and CRMP2 interact to coordinate cytoskeleton dynamics, regulating growth cone development and axon elongation. Neural Plast. 2015, 947423.
Venkatesh, K., Chivatakarn, O., Sheu, S.S., Giger, R.J., 2007. Molecular dissection of the myelin-associated glycoprotein receptor complex reveals cell type-specific mechanisms for neurite outgrowth inhibition. J. Cell Biol. 177, 393–399.
Wang, L.H., Strittmatter, S.M., 1996. A family of rat CRMP genes is differentially expressed in the nervous system. J. Neurosci. 16, 6197–6207.
Witte, H., Neukirchen, D., Bradke, F., 2008. Microtubule stabilization specifies initial neuronal polarization. J. Cell Biol. 180, 619–632.
Yamashita, T., Tohyama, M., 2003. The p75 receptor acts as a displacement factor that releases Rho from Rho-GDI. Nat. Neurosci. 6, 461–467.
Yuki, N., Hartung, H.P., 2012. Guillain–Barre syndrome. N. Engl. J. Med. 366, 2294–2304.
Zhang, Y., Yu, L.C., 2008. Microinjection as a tool of mechanical delivery. Curr. Opin. Biotechnol. 19, 506–510.
Zhang, G., Lopez, P.H., Li, C.Y., Mehta, N.R., Griffin, J.W., Schnaar, R.L., Sheikh, K.A., 2004. Anti-ganglioside antibody-mediated neuronal cytotoxicity and its protection by intravenous immunoglobulin: implications for immune neuropathies. Brain 127, 1085–1100.
Zhang, G., Lehmann, H.C., Manoharan, S., Hashmi, M., Shim, S., Ming, G.L., Schnaar, R.L., Lopez, P.H., Bogdanova, N., Sheikh, K.A., 2011. Anti-ganglioside antibody-mediated activation of RhoA induces inhibition of neurite outgrowth. J. Neurosci. 31, 1664–1675.